

# 磁浮導引系統之多輸入多輸出適應滑差模式控制器設計

## GUIDANCE CONTROL CHARACTERISTICS FOR A MAGLEV SYSTEM WITH MIMO ADAPTIVE SLIDING MODE CONTROLLER

陳美勇\* 王晉中\*\* 傅立成†

Mei-Yung Chen Chin-Chung Wang Li-Chen Fu

\*國立台灣大學電機工程研究所      \*\*揚智科技股份有限公司      †國立台灣大學電機及資訊工程學系  
\*Ph.D.      \*\*Senior Engineer      †Professor  
\*Department of Electrical Engineering, National Taiwan University, Taipei, Taiwan 10617, R.O.C.  
\*\*ALi Corporation, Taipei 114, Taiwan  
†Dept. of Computer Science and Information Electrical Engineering, National Taiwan University,  
Taipei, Taiwan 10617, R.O.C.

### 摘要

本研究實現了一套雙軸架構之磁浮定位平台，此平台是雙層架構且由兩個單軸之定位平台組合而成。首先，本研究針對此系統推導出完整之導引動態模型，並基於此動態模型在系統參數未知之狀況下，設計一多輸入多輸出之適應滑差模式控制器用以控制此定位平台之運動姿態。經由實驗結果證實：本研究設計之磁浮定位平台具有高剛度與高解析度之特性，並且與理論分析之結果相符合。

**關鍵詞：** 磁浮導引、混成磁鐵、適應滑差模式控制器。

### Abstract

In this paper, a prototype of a double-deck electromagnet levitated guiding platform is proposed and implemented. It is a repulsive maglev system consisting of two single-axis guiding sub-systems. First of all, the dynamic model of the overall system with complete DOFs (degree-of-freedoms) for guidance is derived and analyzed thoroughly. Next, a MIMO adaptive sliding mode controller which deals with the unknown parameters is well designed to regulate the attitude in this system. From experimental results, the high performance in terms of stiffness and resolution has been demonstrated, which quite matches the theoretical performance.

**Keywords:** Maglev guiding, hybrid magnet, adaptive sliding mode controller.

## 1. INTRODUCTION

Up to now, high precision planar short-range motion platform is widely adopted in the tremendously booming electronics and/or semiconductor industries. However, this kind of machine device normally needs to work in a very clean environment. With need of such particular feature requirement, a larger class of traditional ball-screw type motion platform may not suffice. Therefore, a technology with special kind of actuation subject to some special kind of bearing will then be called for to build the aforementioned device.

Nowadays, maglev levitation has spanned many fields, and large volume of literature has been published. Some well known fields include maglev transportation [1,2], wind tunnel levitation [3], magnetic bearings [4], and anti-vibration tables [5]. Here, however, we will

only investigate the maglev techniques for the field of short-range travel with precision positioning and then design and implement a prototype maglev system to verify its high performance.

Especially electronics and/or in semiconductor industry, high precision positioning is one of the most important technologies in all the manufacturing process. These reasons motivate us to design linear magnetic bearing in conjunction with linear motor (modified voice coil motor will be chosen) to achieve the high-precision positioning purpose.

In our foregoing research [6-10], we have analyzed the dynamics of a single-axis maglev guiding system and derived its analytical model. The basic concept for system set-up can be referred back to the work by Wang [11]. In this paper, a more general dual-axis maglev guiding system is built, based on the above-mentioned

works. Then, an effective adaptive controller which deals with the unknown parameters is proposed to achieve goals of accurate guiding. Experimental results are provided to demonstrate the feasibility of such dual-axis set-up and the effectiveness of the developed controller.

The paper is divided into five sections. In Section 2, the overall system is described and a complete dynamics of the overall system is derived based on detail calculation of the magnetic force functions involved in our set-up and various operating points needed for subsequent linearization. In Section 3, a MIMO adaptive sliding mode controller is proposed to solve the control problem subject to unknown system parameters. Experimental set-up and results with discussion are presented in the following Section 4. Finally, some conclusions are drawn in Section 5.

## 2. SYSTEM DESCRIPTION AND MODELING

The set-up of the dual-axis maglev system consists of gap sensors, voice coil motor (VCM) [10], levitators and stabilizers, which can generate identical flux distribution along the tracks. The perspective and top view of the dual-axis maglev system are shown in Figs. 1 and 2. The carrier moves along the upper guiding tracks in the  $Y$ -axis, whereas the upper guiding tracks moves along the lower guiding tracks in the  $X$ -axis. The upper guiding tracks levitate the carrier, and the carrier and the upper guiding tracks as a whole is called upper position system. Similarly, the lower guiding tracks levitate the upper guiding tracks, and the lower guiding tracks together with the upper guiding tracks is referred to as the lower guiding system.

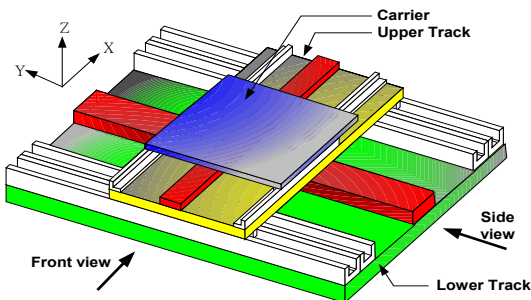


Fig. 1 Perspective of whole maglev system

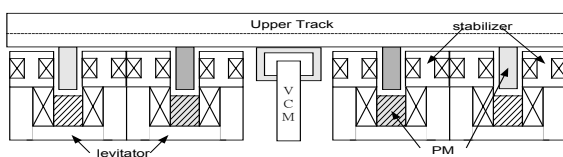


Fig. 2 The side view of lower guiding system

In carrier design, let the  $xyz$  coordinate system be fixed on the carrier and the  $XYZ$  coordinate system be fixed on the upper track. If these two coordinate systems coincide initially, an arbitrary orientation of the  $xyz$  coordinate system can be described in Fig. 3.

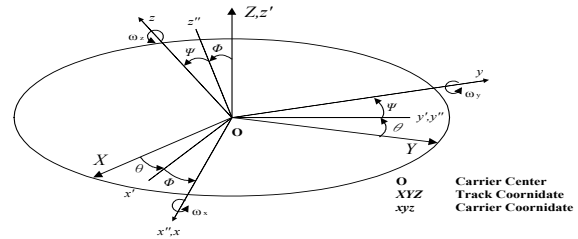


Fig. 3 Eulerian angles

where  $\theta$ ,  $\phi$  and  $\psi$  are Eulerian angles of the  $xyz$  coordinate system. The transformation from  $xyz$ -coordinate to  $XYZ$ -coordinate can be obtained by performing matrix multiplication of the individual rotation matrices  $T$ .

In order to achieve the goal of high-precision guiding, we must control translation and attitude of the carrier. To achieve this purpose, a complete analytical model, which includes four lateral DOFs, two propulsion DOFs and six vertical DOFs, will be derived and analyzed thoroughly. Before we proceed with the modeling task, several technical assumptions must be stated.

- (a) The  $n$ -turn wires of the stabilizing and the levitating coils, which normally come in pairs, are stowed in the coil frames primly. Each side of the single turn loop wire is viewed as an equivalent long straight current-carrying wire which is parallel to all the other wires.
- (b) Each magnet is made of NdFeB characterized by uniform magnetization.
- (c) The tracks are relatively long with respect to the travel range of the carrier, so that all the levitation magnets only undergo uniform magnetic fields along the track.

Consider the carrier to be represented by a uniform box shaped object with the center of mass coincident with the center of geometry. The principle of linear momentum leads to the following equations:

$$F_x = m \ddot{x}, \quad F_y = m \ddot{y}, \quad F_z = m \ddot{z} \quad (1)$$

where  $F_x$ ,  $F_y$  and  $F_z$  are the resultant forces acting on the carrier along the  $X$ -axis,  $Y$ -axis and  $Z$ -axis, respectively, and  $m$  is the mass of the carrier.

By the same token, the principle of angular momentum leads to torque equations for the rotational coordinates. Form Euler's equations [12], the dynamics of the rotation variables all with respect to the carrier

coordinate can be described as follows:

$$\begin{aligned} T_x &= I_{xx} \dot{\omega}_x + (I_{zz} - I_{yy}) \omega_y \omega_z \\ T_y &= I_{yy} \dot{\omega}_y + (I_{xx} - I_{zz}) \omega_x \omega_z \\ T_z &= I_{zz} \dot{\omega}_z + (I_{yy} - I_{xx}) \omega_x \omega_y \end{aligned} \quad (2)$$

where  $T_x$ ,  $T_y$  and  $T_z$  are the external torques  $I_{xx}$ ,  $I_{yy}$  and  $I_{zz}$  are the principal moments of inertia, and  $\omega_x$ ,  $\omega_y$  and  $\omega_z$  are the three angular velocities of the rigid body.

The equations of force and torque on a magnet induced by an infinitely long current-carrying straight wire can be rewritten as in the following forms suitable which are the most relevant to this maglev system [8]:

$$F_x(x, z, I) = \frac{m_z \mu_0 I}{2\pi} \frac{(z^2 - x^2)}{(x^2 + z^2)^2} \quad (3)$$

$$F_z(x, z, I) = \frac{m_z \mu_0 I}{2\pi} \frac{-2xz}{(x^2 + z^2)^2} \quad (4)$$

$$T(x, z, I) = \frac{m_z \mu_0 I}{2\pi} \frac{z}{x^2 + z^2} \hat{k} \equiv T(x, z, I) \hat{k} \quad (5)$$

The forces and torque acting on the levitation magnet are from levitators and stabilizers. The notation of  $m_z$  is the dipole moment of infinitesimal current loop,  $\mu_0$  is the permeability of free space, and  $I$  is input current.

Before formulating equations of motion, some notations on force and torque are explained in the following: the subscript has three letters, the first means the direction of force, the second is magnet location, and the last means the coefficient for state or input, e.g.,  $K_{XAZ}$  is the coefficient of the force on magnet  $A$  in the  $X$ -direction associated with vertical displacement  $\delta z$ ,  $K_{XAZ}$  is the coefficient of the force on magnet  $A$  in  $X$ -direction associated with input current from stabilization coil, and  $K_{ZAI}$  is the coefficient of the force on magnet  $A$  in  $Z$ -direction associated with input current from levitation coil. Then, each permanent magnet is exerted by two magnetic forces, namely,  $F_{XA}$ ,  $F_{ZA}$  and  $T_{YA}$ , which can be linearized as in the following equations:

$$F_{XA} = K_{XAX} \delta x + K_{XAZ} \delta z + K_{XAs} \delta I \quad (6)$$

$$F_{ZA} = K_{ZAX} \delta x + K_{ZAZ} \delta z + K_{ZAI} \delta I \quad (7)$$

$$T_{YA} = K_{YAX} \delta x + K_{YAI} \delta I \quad (8)$$

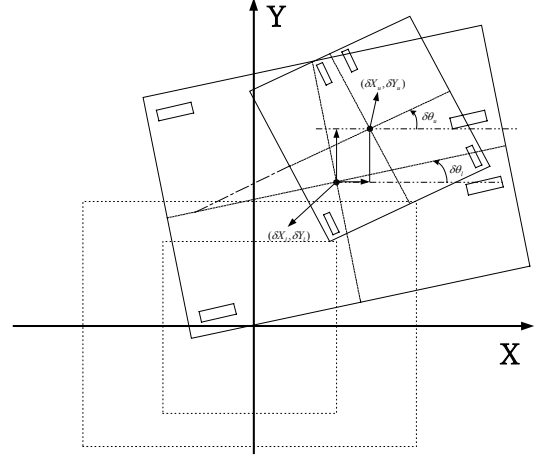


Fig. 4 Top view of Maglev guiding system

The locations of the levitation magnets are shown in Fig. 5. Combine these small displacement (the subscript  $u$  denotes carrier and  $l$  denote signals concerning the upper track) with Eq. (6) to Eq. (8), we can derive the interaction force between a magnet and a track. By means of magnetic force functions, the complete set of analytical equations of motion can be obtained (More detailed modeling process and parameter definitions can be found in [14]) as:

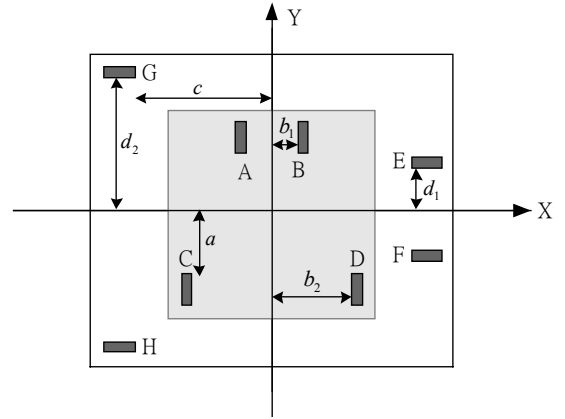


Fig. 5 Position of the eight levitation magnets

A. Upper track

$$\begin{aligned} F_{X\_total} &= m \ddot{X}_l = 4K_{XEX} X_l \\ &\quad + 4K_{XEZ} Z_l + 2K_{XEs} I_{l1} + 2K_{XEs} I_{l2} \\ &\quad - K_{u6} V_{u6} + c_{u6} \dot{Y}_u | \dot{Y}_u | + b_{u6} (1 + a_{u6}^2 Y_u^2) Y_u \\ F_{Y\_total} &= m \ddot{Y}_l = F_Y + (F_{XA} + F_{XB} + F_{XC} + F_{XD}) \\ &= K_6 V_{l6} - c_6 \dot{Y}_l | \dot{Y}_l | - b_6 (1 + a_6^2 Y_l^2) Y_l \\ &\quad + 4K_{XAX} X_u + 4K_{XAZ} Z_u + 2K_{XAs} I_{u1} + 2K_{XAs} I_{u2} \end{aligned}$$

$$\begin{aligned}
F_{Z\_total} &= m\ddot{Z}_l = (F_{ZE} + F_{ZF} + F_{ZG} + F_{ZH}) \\
&\quad - (F_{ZA} + F_{ZB} + F_{ZC} + F_{ZD}) \\
&= 4K_{ZEX}X_l + 4K_{ZYZ}Z_l + 2K_{ZEI}I_{l4} + K_{ZEI}I_{l3} \\
&\quad + K_{ZEI}I_{l5} - 4K_{ZAX}X_u - 4K_{ZAZ}Z_u \\
&\quad - 2K_{ZAI}I_{u4} - K_{ZAI}I_{u3} - K_{ZAI}I_{u5}
\end{aligned}$$

$$\begin{aligned}
T_{X\_total} &= J_X\ddot{\psi}_l = 4c^2K_{ZEX}\theta_l \\
&\quad + 4c^2K_{ZYZ}\psi_l + 2cK_{ZEI}I_{l4} - cK_{ZEI}I_{l3} - cK_{ZEI}I_{l5} \\
&\quad - 2b_2^2K_{ZAZ}\phi_u + b_2K_{ZAI}I_{u3} - b_2K_{ZAI}I_{u5}
\end{aligned}$$

$$\begin{aligned}
T_{Y\_total} &= J_Y\ddot{\phi}_l = d_2(F_{ZH} - F_{ZG}) \\
&\quad - [(Y_u + a)(F_{ZA} + F_{ZB}) + (Y_u - a)(F_{ZC} + F_{ZD})] \\
&= 2d_2^2K_{ZYZ}\phi_l + d_2K_{ZEI}I_{l3} - d_2K_{ZEI}I_{l5} \\
&\quad + 4a^2K_{ZAX}\theta_u + 4a^2K_{ZAZ}\psi_u + 2aK_{ZAI}I_{u4} \\
&\quad - aK_{ZAI}I_{u3} - aK_{ZAI}I_{u5}
\end{aligned}$$

$$\begin{aligned}
T_{Z\_total} &= J_Z\ddot{\theta}_l \\
&= c[(F_{XE} + F_{XF}) - (F_{XG} + F_{XH})] \\
&\quad - a[(F_{XA} + F_{XB}) - (F_{XC} + F_{XD})] \\
&= 4c^2K_{XEX}\theta_l + 4c^2K_{XEZ}\psi_l + 2cK_{XES}I_{l1} \\
&\quad + 2cK_{XES}I_{l2} - 4a^2K_{XAX}\theta_u - 2aK_{XAS}I_{u1} \\
&\quad + 2aK_{XAS}I_{u2} - 4Y_uK_{XAX}X_u - 4aY_uK_{XAZ}\psi_u \\
&\quad - 4Y_uK_{XAZ}Z_u - 2Y_uK_{XAS}I_{u1} - 2Y_uK_{XAS}I_{u2} \quad (9)
\end{aligned}$$

### B. Carrier

$$\begin{aligned}
F_{uX\_total} &= m_u\ddot{X}_u = (F_{XA} + F_{XB} + F_{XC} + F_{XD}) - F_Y \\
&= 4K_{XAX}X_u + 4K_{XAZ}Z_u + 2K_{XAS}I_{u1} + 2K_{XAS}I_{u2} \\
&\quad - K_6V_{l6} + c_6\dot{Y}_l | \dot{Y}_l | + b_6(1 + a_6^2Y_l^2)Y_l
\end{aligned}$$

$$\begin{aligned}
F_{uY\_total} &= m_u\ddot{Y}_u = F_{uY} + (F_{XE} + F_{XF} + F_{XG} + F_{XH}) \\
&= K_{u6}V_{u6} - c_{u6}\dot{Y}_u | \dot{Y}_u | - b_{u6}(1 + a_{u6}^2Y_u^2)Y_u \\
&\quad + 4K_{XEX}X_l + 4K_{XEZ}Z_l + 2K_{XES}I_{l1} + 2K_{XES}I_{l2}
\end{aligned}$$

$$\begin{aligned}
F_{uZ\_total} &= m_u\ddot{Z}_u = (F_{ZA} + F_{ZB} + F_{ZC} + F_{ZD}) \\
&\quad + (F_{ZE} + F_{ZF} + F_{ZG} + F_{ZH}) \\
&= 4K_{ZAX}X_u + 4K_{ZAZ}Z_u + 2K_{ZAI}I_{u4} + K_{ZAI}I_{u3} \\
&\quad + K_{ZAI}I_{u5} + 4K_{ZEX}X_l + 4K_{ZYZ}Z_l + 2K_{ZEI}I_{l4} \\
&\quad + K_{ZEI}I_{l3} + K_{ZEI}I_{l5}
\end{aligned}$$

$$T_{uX\_total} = T_{uX} - T_Y = a[(F_{ZA} + F_{ZB}) - (F_{ZC} + F_{ZD})]$$

$$\begin{aligned}
&- d_2(F_{ZH} - F_{ZG}) = 4a^2K_{ZAX}\theta_u + 4a^2K_{ZAZ}\psi_u \\
&\quad + 2aK_{ZAI}I_{u4} - aK_{ZAI}I_{u3} - aK_{ZAI}I_{u5} \\
&\quad - 4Y_uK_{ZEX}X_l - 4cY_uK_{ZYZ}\psi_l - 4Y_uK_{ZYZ}Z_l \\
&\quad - 2Y_uK_{XES}I_{l1} - 2Y_uK_{XES}I_{l2}
\end{aligned}$$

$$\begin{aligned}
T_{uY\_total} &= J_{uY}\ddot{\phi}_u \\
&= b_2(F_{ZD} - F_{ZC}) + c[(F_{ZG} + F_{ZH}) - (F_{ZE} + F_{ZF})] \\
&= 2b_2^2K_{ZAZ}\phi_u + b_2K_{ZAI}I_{u3} - b_2K_{ZAI}I_{u5} \\
&\quad - 4c^2K_{ZEX}\theta_l - 4c^2K_{ZYZ}\psi_l - 2cK_{ZEI}I_{l4} \\
&\quad + cK_{ZEI}I_{l3} + cK_{ZEI}I_{l5} \\
T_{uZ\_total} &= J_{uZ}\ddot{\theta}_u = a[(F_{XA} + F_{XB}) - (F_{XC} + F_{XD})] \\
&\quad + c[(F_{XE} + F_{XF}) - (F_{XG} + F_{XH})] \\
&\quad + 4a^2K_{XAX}\theta_u + 4a^2K_{XAZ}\psi_u + 2aK_{XAS}I_{u1} \\
&\quad - 2aK_{XAS}I_{u2} + m\ddot{Y}_u + 4a^2K_{XEX}\theta_l \\
&\quad + 4c^2K_{XEZ}\psi_l + 2cK_{XES}I_{l1} - 2cK_{XES}I_{l2} \quad (10)
\end{aligned}$$

## 3. CONTROLLER DESIGN AND STABILITY ANALYSIS

In the previous section, though complete derivation of model is described, we have made several assumptions, which will inevitably result in modeling errors. Therefore, the controller to be developed should be robust enough to tolerate these system uncertainties and unmodeled dynamics. Besides these uncertainties, the controller also has to eliminate the effect due to disturbances. In this paper, we adopt an adaptive controller for the task of dual-axis maglev system.

### 3.1 Controller Design

In order to obtain a compact controller, redefine the control inputs as

$$\begin{aligned}
\begin{bmatrix} u_1 \\ u_2 \end{bmatrix} &= \begin{bmatrix} 50 & 50 \\ R_{l1} & R_{l2} \end{bmatrix} \begin{bmatrix} V_{l1} \\ V_{l2} \end{bmatrix} \\
\begin{bmatrix} u_3 \\ u_4 \\ u_5 \end{bmatrix} &= \begin{bmatrix} 25 & 50 & 25 \\ R_{l3} & R_{l4} & R_{l5} \\ 25 & 0 & -25 \\ R_{l3} & & R_{l5} \\ -25 & 50 & -25 \\ R_{l3} & R_{l4} & R_{l5} \end{bmatrix} \begin{bmatrix} V_{l3} \\ V_{l4} \\ V_{l5} \end{bmatrix} \quad (11)
\end{aligned}$$

$$\begin{bmatrix} u_6 \\ u_7 \end{bmatrix} = \begin{bmatrix} \frac{50}{R_{u1}} & \frac{50}{R_{u2}} \\ \frac{50}{R_{u1}} & -\frac{50}{R_{u2}} \end{bmatrix} \begin{bmatrix} V_{u1} \\ V_{u2} \end{bmatrix}$$

$$\begin{bmatrix} u_8 \\ u_9 \\ u_{10} \end{bmatrix} = \begin{bmatrix} \frac{25}{R_{u3}} & \frac{50}{R_{u4}} & \frac{25}{R_{u5}} \\ \frac{25}{R_{u3}} & 0 & -\frac{25}{R_{u5}} \\ -\frac{25}{R_{u3}} & \frac{50}{R_{u4}} & -\frac{25}{R_{u5}} \end{bmatrix} \begin{bmatrix} V_{u3} \\ V_{u4} \\ V_{u5} \end{bmatrix} \quad (12)$$

According to these definitions, we rewrite Eq. (9) and Eq. (10) into state-space form as:

$$M\ddot{E} = AE + BU + CG + DH + W \quad (13)$$

where  $E$  is state variable vector,  $U$  is control input,  $G$  and  $H$  are nonlinear terms which are caused by platform moving. The external disturbances and high order terms resulting from linearization are modeled as a column vector,  $W$ . Besides, there are four primary factors that account for uncertainties. Additionally,  $v$  are modeled here in order to cancel the sensor calibration error. These errors are due to the mismatches of the actual neutral points (tracks) and the set neutral points (sensors). Rewrite the Eqs. (13)

$$D_B \ddot{E} = -D_A E + U + v \quad (14)$$

where

$$E = [X_l \ \theta_l \ Z_l \ \phi_l \ \psi_l \ X_u \ \theta_u \ Z_u \ \phi_u \ \psi_u]^T$$

$$U = [u_1 \ \cdots \ u_{10}]^T, v = [v_1 \ \cdots \ v_{10}]^T$$

$$D_A = \text{diag}(a_{11}, a_{22}, \dots, a_{1010}), D_B = \text{diag}(b_{11}, b_{22}, \dots, b_{1010})$$

Thus, a compact form of the overall system model is derived.

We assume a sliding surface  $S$ , which satisfies:

$$S = G_D \dot{E} + G_P E \quad (15)$$

where  $G_D = [\lambda_{d1} \ \lambda_{d2} \ \cdots \ \lambda_{d10}]^T$ ,  $G_P = [\lambda_{p1} \ \lambda_{p2} \ \cdots \ \lambda_{p10}]^T$ ,  $\lambda_{di} > 0$  and  $\lambda_{pi} > 0$ ,  $\forall i = 1 \sim 10$ , and we find that  $S$  depends on error column vector  $E$  and its time derivatives. For our applications, we are to regulate every entry in the error column vector  $E$  to zero. In the mean time, the time derivatives of every entry in  $E$ , which are denoted as  $\dot{E}$ , also have to be regulated to zero to ensure the errors included in column vector  $E$  stay at zero. Due to this reason, if we can prove the sliding surface tends to zero within finite time, then we

can assure  $E$  and  $\dot{E}$  also are forced to zero exponentially. To relate the sliding surface to the dynamics of motion, we find out the time derivative of the sliding surface is:

$$\dot{S} = G_D \ddot{E} + G_P \dot{E} \quad (16)$$

As described in the previous section, we apply an adaptive controller here, which is capable of estimating parameters of system on-line and controlling the system simultaneously. After we have the estimates of system parameters, we can use Eq. (16) with these estimates in the control command. So, we substitute the estimates acquired from the on-line estimator and derive the following:

$$U = \hat{D}_B G_D^{-1} (-K G_D \dot{E} - K G_P E - G_P E) + \hat{D}_A E - \hat{G} - \hat{v} - \text{sat}(S) \quad (17)$$

where  $\hat{D}_B$ ,  $\hat{D}_A$ ,  $\hat{G}$ , and  $\hat{v}$  are the estimates of  $D_B$ ,  $D_A$ ,  $G$ , and  $v$ , respectively, and  $K = [k_1 \ k_2 \ \cdots \ k_{10}]^T$ ,  $k_i > 0$ ,  $\forall i = 1 \sim 10$ ,

$$\text{sat}(S) = \text{sat}([s_1 \ s_2 \ \cdots \ s_{10}]^T), s_i = \begin{cases} 1 & s_i > \varepsilon_i \\ \frac{s_i}{|\varepsilon_i|} & \text{if } \varepsilon_i \geq s_i \geq -\varepsilon_i \\ -1 & s_i < -\varepsilon_i \end{cases}$$

Thus, substituting Eq. (17) into Eq. (15), we can obtain

$$D_B [G_D^{-1} \dot{S} + K (G_D^{-1} S)] = -\tilde{D}_A E + \tilde{G} + \tilde{v} + \tilde{D}_B (-K G_D^{-1} S - G_D^{-1} G_P E) - \text{sat}(S) \quad (18)$$

where the estimation errors are defined as  $\tilde{D}_B = D_B - \hat{D}_B$ ,  $\tilde{D}_A = D_A - \hat{D}_A$ ,  $\tilde{G} = G - \hat{G}$  and  $\tilde{v} = v - \hat{v}$ . By applying appropriate  $K$ ,  $G_D$  and  $G_P$ , we can accelerate the convergence and force them to zero in a shorter period of time.

### 3.2 Adaptive Laws

In the previous section, we have derived the close-loop function in Eq. (18), which involves estimation errors. Now, with the help of estimator based on adaptive control theory, then we can derive the estimates, so that appropriate control commands are also derived.

We define a Lyapunov function candidate  $V$ , which is a positive definite function:

$$\begin{aligned}
V &= \frac{1}{2} \{ [D_B(G_D^{-1}S)]^T [D_B(G_D^{-1}S)] \\
&+ tr [(\tilde{D}_A)^T D_B \Gamma_3^{-1} (\tilde{D}_A)] + tr [(\tilde{D}_B)^T D_B \Gamma_4^{-1} (\tilde{D}_B)] \\
&+ tr [(\tilde{G})^T D_B \Gamma_5^{-1} (\tilde{G})] + tr [(\tilde{v})^T D_B \Gamma_6^{-1} (\tilde{v})] \} \quad (19)
\end{aligned}$$

where  $\Gamma_3^{-1}$ ,  $\Gamma_4^{-1}$ ,  $\Gamma_5^{-1}$ ,  $\Gamma_6^{-1}$ , are all positive diagonal matrixes. First, we find out the time derivative of the Lyapunov candidate function  $V$  as:

$$\begin{aligned}
\dot{V} &= [D_B(G_D^{-1}S)]^T [D_B(G_D^{-1}\dot{S})] \\
&+ tr [(\tilde{D}_A)^T D_B \Gamma_3^{-1} (\dot{\tilde{D}}_A)] + tr [(\tilde{D}_B)^T D_B \Gamma_4^{-1} (\dot{\tilde{D}}_B)] \\
&+ tr [(\tilde{G})^T D_B \Gamma_5^{-1} (\dot{\tilde{G}})] + tr [(\tilde{v})^T D_B \Gamma_6^{-1} (\dot{\tilde{v}})] \quad (20)
\end{aligned}$$

along the solution trajectory of  $S$  in Eq. (15). Then, it can be rearranged by means of Eq. (20) into the following:

$$\begin{aligned}
\dot{V} &= -[D_B(G_D^{-1}S)]^T [D_B K(G_D^{-1}S)] \\
&- [D_B(G_D^{-1}S)]^T [D_B G_D^{-1} sat(S)] \\
&+ tr [(\tilde{D}_A)^T D_B \Gamma_3^{-1} (\dot{\tilde{D}}_A) - (\tilde{D}_A)^T D_B (G_D^{-1}S) E^T] \\
&+ tr [(\tilde{D}_B)^T D_B \Gamma_4^{-1} (\dot{\tilde{D}}_B) + (\tilde{D}_B)^T D_B (G_D^{-1}S) \\
&\cdot (-K G_D^{-1}S - G_D^{-1} G_P \dot{E})^T] \\
&+ tr [(\tilde{G})^T D_B \Gamma_5^{-1} (\dot{\tilde{G}}) + (\tilde{G})^T D_B \Gamma_5^{-1} (G_D^{-1}S)] \\
&+ tr [(\tilde{v})^T D_B \Gamma_6^{-1} (\dot{\tilde{v}}) + (\tilde{v})^T D_B (G_D^{-1}S)] \quad (21)
\end{aligned}$$

Now, we choice adaptive laws as follow:

$$\begin{aligned}
\dot{\tilde{D}}_A &= -\dot{\tilde{D}}_A = -\Gamma_3 (G_D^{-1}S) E^T \\
\dot{\tilde{D}}_B &= -\dot{\tilde{D}}_B = \Gamma_4 (G_D^{-1}S) (-K G_D^{-1}S - G_D^{-1} G_P \dot{E})^T \\
\dot{\tilde{G}} &= -\dot{\tilde{G}} = \Gamma_5 (G_D^{-1}S) \\
\dot{\tilde{v}} &= -\dot{\tilde{v}} = \Gamma_6 (G_D^{-1}S) \quad (22)
\end{aligned}$$

If these equations hold, Eq. (21) will become

$$\begin{aligned}
\dot{V} &= -S^T G_D^{-1} D_B^T D_B K G_D^{-1} S \\
&- S^T G_D^{-1} D_B^T D_B G_D^{-1} sat(S) \leq 0 \\
&= \begin{cases} -S^T G_D^{-1} D_B^T D_B K G_D^{-1} S - \sum_{i=1}^{12} k_i |s_i| \leq 0 & |s_i| > \varepsilon_i \\ -S^T G_D^{-1} D_B^T D_B K G_D^{-1} S - \sum_{i=1}^{12} k_i \frac{s_i^2}{|\varepsilon_i|} \leq 0 & |s_i| \leq \varepsilon_i \end{cases} \quad (23)
\end{aligned}$$

because  $G_D^{-1}$ ,  $G_B$  and  $K$  are all positive diagonal matrices so that they are commutable in deriving the inequality. And Eq. (23) also implies that the equilibrium  $D_A = \hat{D}_A$ ,  $D_B = \hat{D}_B$ ,  $G = \hat{G}$  and  $v = \hat{v}$  of the respective equations is uniformly bounded. Using arguments similar to Lyapunov theory we establish that  $S \in L_2$ ,  $\dot{S} \in L_\infty$  and that:  $|S(t)| \rightarrow 0$ ,  $\|\tilde{D}_A\| \rightarrow 0$ ,  $\|\tilde{D}_B\| \rightarrow 0$ ,  $\|\tilde{G}\| \rightarrow 0$  and  $\|\tilde{v}\| \rightarrow 0$  as  $t \rightarrow \infty$ .

Due to zero convergence of  $S$ , it can be readily verified that every entry in column vector  $E$  coverage to zero asymptotically. In other words, state variables and their time derivatives all converge to zero eventually, which is the goal of designing the controller for this system.

## 4. EXPERIMENTAL RESULTS

The design of overall system is thoroughly described in Section 2. Figure 6 shows the photographs of the physical set-up.

A number of experimental results including the transient and the steady-state responses will be provided in this section to demonstrate the performance of this system with controller presented in Section 3. Based on these results, we will make some conclusions which are important for the future work of this research.

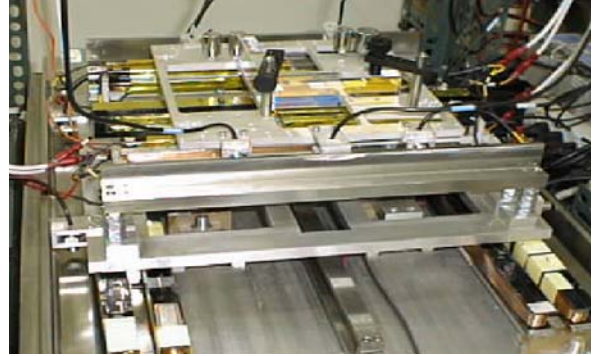


**Fig. 6 Photograph of an aspect of the physical system**

From experimental results show in Figs. 7 and 8, we can observe that the carrier has oscillation in transient response part. It is cause of system magnetic line of force coupling between carrier and upper track. In the system steady state part, carrier guiding resolution is  $1 \times 10^{-5}$  m and upper track guiding resolution is  $3 \times 10^{-5}$  m. We list the experimental data here. These experimental data reveal that adaptive controller successfully regulate all the attitudes of the dual-axis maglev system.

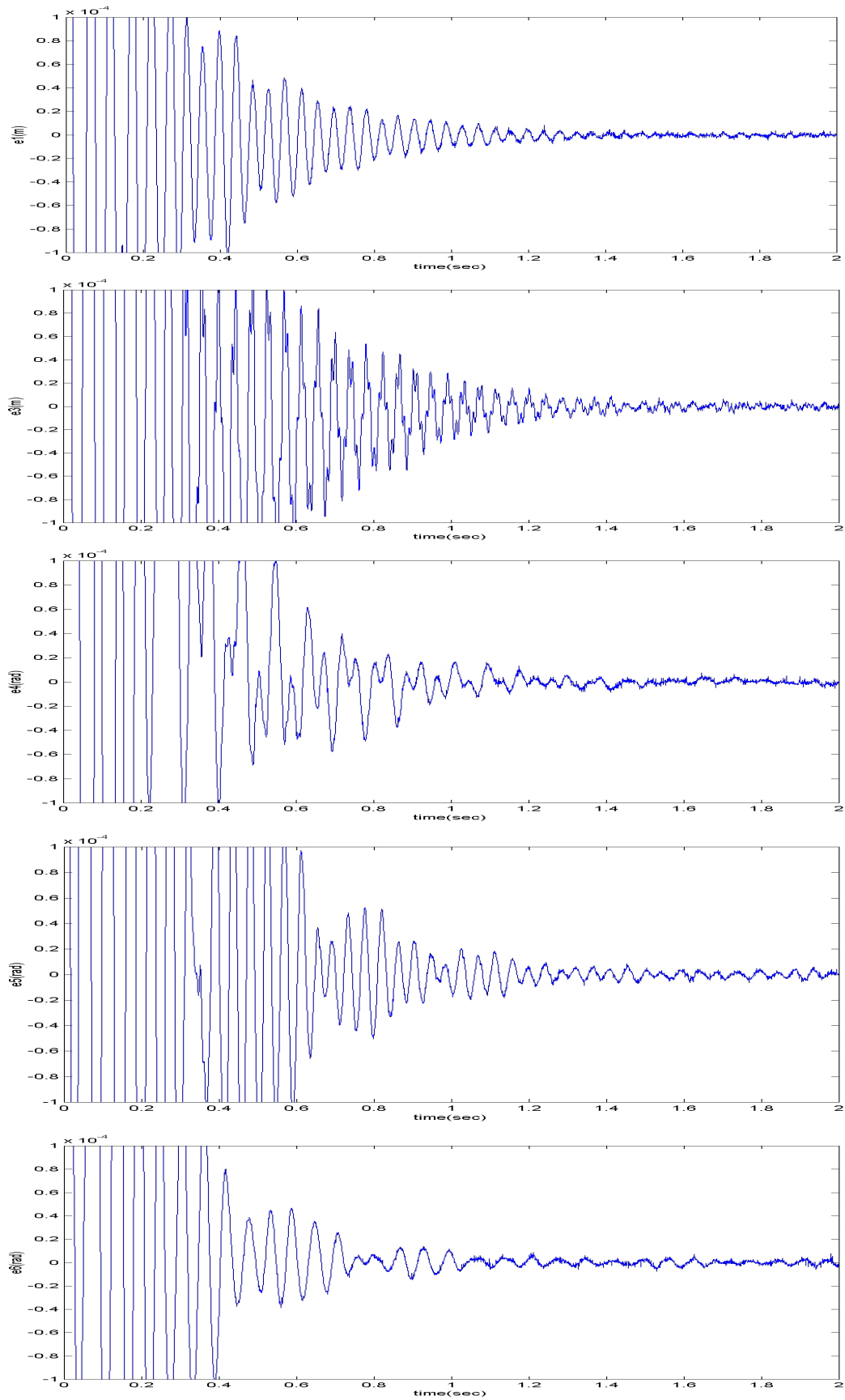


**Fig. 7** System transient and steady state response of carrier

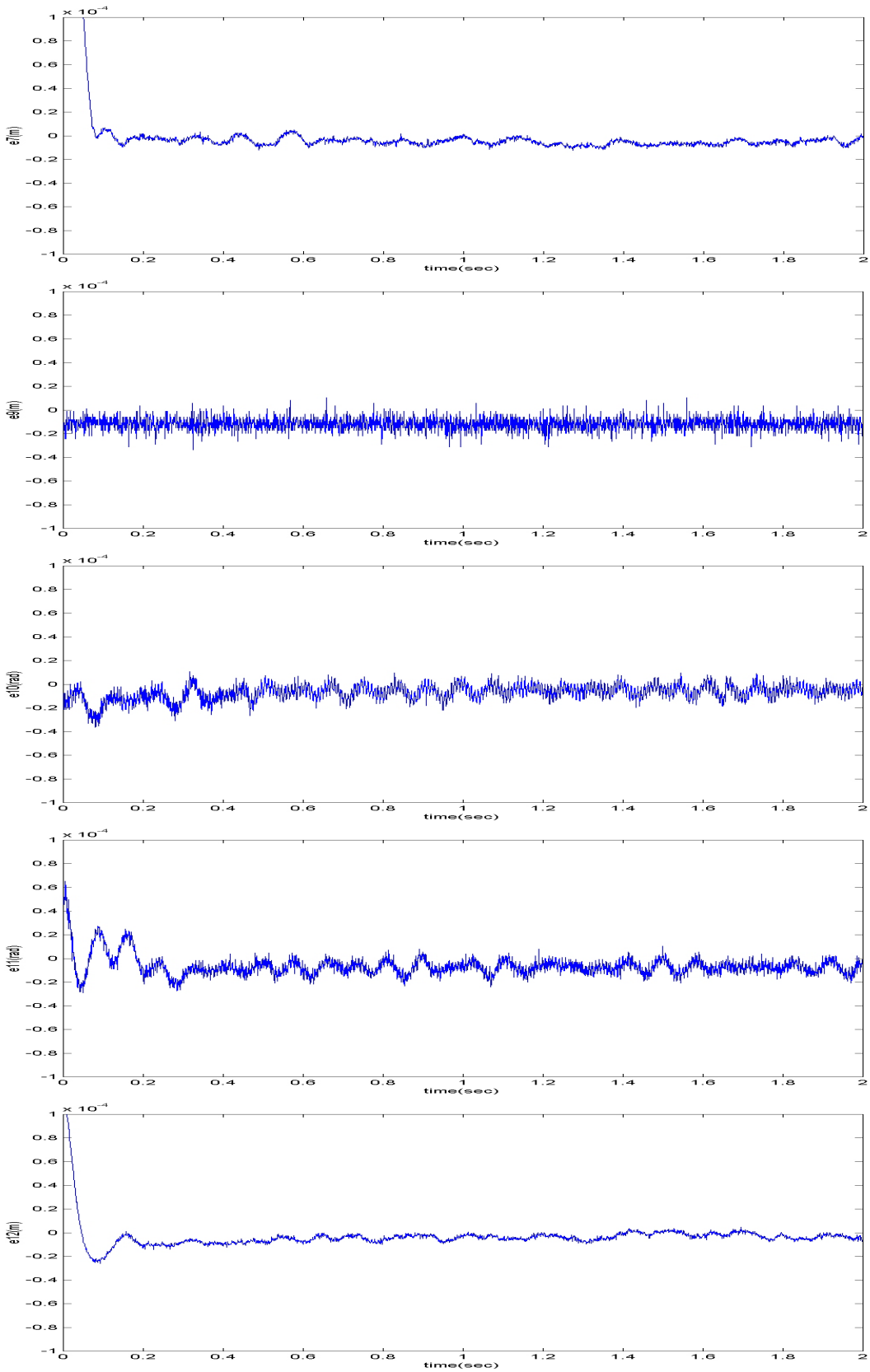


Fig. 8 System transient and steady state response of upper track

## 5. CONCLUSION

Throughout the research presented in this paper, a dual-axis maglev guiding platform was proposed, and a stabilizing and levitating of the system controller is well developed. The dynamics of the guiding system have been analyzed and then its model is also derived. An adaptive controller is designed here because the systems parameters are difficult to know precisely in such a system. From the experimental results, the feasibility and effectiveness have been demonstrated. Moreover, by fixing permanent magnets into tracks as levitation devices, the power consumption of this system is considerably saved. A novel power-saving and high precision guiding maglev X-Y table is successfully accomplished.

## ACKNOWLEDGEMENT

This research is sponsored by National Science Council, R.O.C., under the grant NSC 88-2213-E-002-084.

## REFERENCES

- [1] B. V. Jayawant, P. K. Sinha and D. G. Aylwin, "Feedback control system for D.C. electromagnets in passenger-carrying vehicles," *Int. J. Control*, Vol. 24, No. 5, 1976, pp. 627–639.
- [2] M. Proise, *et al.*, "System concept definition of the grumman superconducting electromagnetic suspension (EMS) maglev design," *Maglev '93 Conf. Argonne National Laboratory*, May 19–21, 1993.
- [3] E. E. Covert, M. Vlajinac, T. Stephens and M. Finston, "Magnetic balance and suspension systems for use with wind tunnels," *Progress in Aerospace Science*, Vol. 14., D, Kuchemann, ed., Pergamon Press, 1973, pp. 27–107.
- [4] H. Bleuler, "A survey of magnetic levitation and magnetic bearing types," *JSME International Journal*, Vol. 35, 1992, pp. 335–342.
- [5] N. Kosuke and I. Masashi, "A noncontact permanent magnet levitation table with electromagnetic control and its vibration isolation method using direct disturbance cancellation combining optimal regulators," *IEEE Tran. on Magnetics*, Vol. 31, No. 1, Jan. 1995.
- [6] M. Y. Chen, K. N. Wu and L. C. Fu, "Adaptive control and experiment of a maglev guiding system for wafer transportation," *I.F.A.C. Workshop on Motion Control Conference*, 1998.
- [7] M. Y. Chen, K. N. Wu and L. C. Fu, "Design, implementation and self-tuning adaptive control of a maglev guiding system," *Mechatronic*, 2000, pp. 215–237.
- [8] M. Y. Chen, M. J. Wang and L. C. Fu, "Modeling and controller design of a maglev guiding system for application in precision positioning," *American Control Conference*, 1999.
- [9] M. Y. Chen, M. J. Wang and L. C. Fu, "Dual-axis maglev guiding system modeling and controller design for wafer transportation," *Control and Decision Conference*, 1999.
- [10] C. C. Wang, M. Y. Chen and L. C. Fu, "Adaptive sliding mode controller design of a maglev guiding system for application in precision positioning," *American Control Conference*, 2000.
- [11] I. Y. Wang, "A magnetic levitation silicon wafer transport system," Doctor Dissertation, The University of Texas at Austin, 1993.
- [12] David L. Trumper, Sean M. Olson and Pradeep K. Subrahmanyam, "Linearizing control of a magnetic suspension systems," *IEEE Tran. on Control Systems Technology*, Vol. 5, No. 4, July 1996.
- [13] Jean-Jacques E. Slotine, Weiping Li., *Applied Nonlinear Control*, Prentice Hall, 1990.
- [14] Chin-Chung Wang, "A dual-axis maglev positioning system," Master Thesis, The National Taiwan University, Taiwan, R.O.C., 2000.



**Mei-Yung Chen (陳美勇)** was born in Maju, Taiwan, R.O.C., in 1966. He received the B.S. degree from TamKang University, Taipei, Taiwan, R.O.C., in 1992, the M.S. degree from Chung Yuan Christian University, Chung-Li, Taiwan, R.O.C., in 1994, and he is currently a Ph.D. student in the Department of Electrical Engineering, National Taiwan University, Taipei, Taiwan, R.O.C.

He is a teaching assistant in the Automatic Control Lab., Department of Electrical Engineering, National Taiwan University, Taipei, Taiwan, R.O.C. His areas of research interest include magnetic levitation technology, positioning and tracking, mechatronics, and control theory and applications.

He is a student member of the IEEE. He is also a member of the Chinese Automatic Control Society. He received the Best Student Paper Award from the Chinese Automatic Control Society in 2001 and 2003.



**Chin-Chung Wang (王晉中)** was born in Tainan, Taiwan, R.O.C., in 1975. He received the B.S. and M.S. degree in Department of Electrical Engineering from National Taiwan University, in 1998 and 2000, respectively.

Since 2000, he has been with ALi Co. as a senior engineer, where he has involved in the analog IC design of phase-lock loop. His research interests include system integration, adaptive control and analog IC PLL circuit design for consumer electronics.



**Li-Chen Fu (傅立成)** was born in Taipei, Taiwan, R.O.C., in 1959. He received the B.S. degree from National Taiwan University, Taipei, R.O.C., in 1981 and the M.S. and Ph.D. degrees from the University of California, Berkeley, in 1985 and 1987, respectively.

Since 1987, he has been a member of the faculty, and is currently a Professor in both the Department of Electrical Engineering and Department of Computer Science and Information Engineering, National Taiwan University, where he also served as the Deputy Director of the Tjing Ling Industrial Research Institute from 1999 to 2001. His research interests include robotics, FMS scheduling, shop floor control, home automation, visual detection and tracking, E-commerce, and control theory and applications. He has been the Editor of the Journal of Control and Systems Technology and an Associate Editor of the prestigious control journal, Automatica. In 1999, he became the Editor-in-Chief of a new control journal, Asian Journal of Control.

Prof. Fu is a senior member of the IEEE Robotics and Automation and IEEE Automatic Control Societies. He is also a member of the Boards of the Chinese Automatic Control Society and Chinese Institute of Automation Engineers. During 1996 ~ 1998 and 2000, he was appointed as a member of the IEEE Robotics and Automation Society AdCom and will serve as the Program Chair of the 2003 IEEE International Conference on Robotics and Automation. He received the Excellent Research Award for the period 1990 ~ 1993 and Outstanding Research Awards in 1995, 1998, and 2000 from the National Science Council, R.O.C. He also received the Outstanding Youth Medal in 1991, the Outstanding Engineering Professor Award in 1995, and the Best Teaching Award in 1994 from the Ministry of Education, the Ten Outstanding Young Persons Award in 1999 of the R.O.C., the Outstanding Control Engineering Award from the Chinese Automatic Control Society in 2000, and the Lee Kuo-Ding Medal from the Chinese Institute of Information and Computing Machinery in 2000.